A Journal of the Gesellschaft Deutscher Chemiker

Angewandte International Edition GDCh Chemie

www.angewandte.org

Accepted Article

Title: Synthesis of Rhodium Complexes with Chiral Diene Ligands via Diastereoselective Coordination and Their Application in the Asymmetric Insertion of Diazo Compounds into E-H Bonds

Authors: Nikita M. Ankudinov, Denis A. Chusov, Yulia V. Nelyubina, and Dmitry Perekalin

To be cited as: *Angew. Chem. Int. Ed.* 10.1002/anie.202105179

Link to VoR: https://doi.org/10.1002/anie.202105179

WILEY-VCH

10.1002/anie.202105179

WILEY-VCH

RESEARCH ARTICLE

Synthesis of Rhodium Complexes with Chiral Diene Ligands via Diastereoselective Coordination and Their Application in the Asymmetric Insertion of Diazo Compounds into E-H Bonds

Nikita M. Ankudinov, Denis A. Chusov, Yulia V. Nelyubina, and Dmitry S. Perekalin*

[a] N. M. Ankudinov, D. A. Chusov, Y. V. Nelyubina, D. S. Perekalin
A.N. Nesmeyanov Institute of Organoelement Compounds, Russian Academy of Sciences
28 Vavilova str., Moscow, Russia
E-mail: dsp@ineos.ac.ru
Supporting information for this article is given via a link at the end of the document

Abstract: A new method for the synthesis of chiral diene rhodium catalysts is introduced. The readily available racemic tetrafluorobenzobarrelene complexes $[(R_2\text{-TFB})RhCl]_2$ were separated into two enantiomers via selective coordination of one of them with the auxiliary *S*-salicyl-oxazoline ligand. One of the resulting chiral complexes with an exceptionally bulky diene ligand $[(R,R\text{-}i\text{Pr}_2\text{-TFB})RhCl]_2$ proved to be an efficient catalyst for the asymmetric insertion of diazoesters into B−H and Si−H bonds giving the functionalized organoboranes and silanes with high yields (79−97%) and enantiomeric purity (87−98% ee). The stereoselectivity of separation via auxiliary ligand and that of the catalytic reaction was predicted by DFT calculations.

Introduction

The development of enantioselective catalysis largely relies on a diversity of the available chiral ligands. Chiral dienes (Scheme 1) have distinct electronic and steric properties which make them effective ligands for many reactions.[1,2] In particular, rhodium complexes with chiral dienes are among the best catalysts for asymmetric addition of arylboronic acids to the enones, imines, and other polar double bonds.[3–5] Although these catalysts have shown a remarkable performance, their accessibility is still rather limited. Only several chiral dienes are readily available via transformations of natural terpenes.[6,7] More typically chiral dienes are obtained via multi-step synthesis involving catalytic asymmetric reactions, such as hydrosilylation[8] or aldol condensation.[9] Moreover, expensive preparative chiral chromatography is necessary for the separation of some of the most effective ligands.[10–12]

Following an interesting alternative approach, racemic diene ligands can be initially coordinated with rhodium and then the resulting complexes can be separated by crystallization of diastereomeric adducts with *R*-binaphthyl-diamine.[13–16] However, it is difficult to predict if this method can be applied for any particular diene because of the unpredictable nature of the crystallization process itself. This motivated us to propose and develop a new approach to the chiral diene complexes based on their diastereoselective coordination with the auxiliary salicyloxazoline ligands. The approach has two important differences from the crystallization method: firstly, only one of two enantiomers coordinates with an auxiliary ligand, and secondly, the selectivity of such coordination can be efficiently predicted before the synthesis by DFT calculations.

The application of this method allowed us to synthesize a series of the new chiral rhodium complexes with unprecedentedly bulky tetrafluorobenzobarrelene ligands. The resulting complexes appeared to be efficient catalysts for the asymmetric insertion of diazo compounds into B−H and Si−H bonds, producing chiral functionalized organoboranes and silanes with 87-98% enantiomeric excess. The origin of enantioselectivity and the concerted mechanism of this reaction were investigated by DFT calculations.

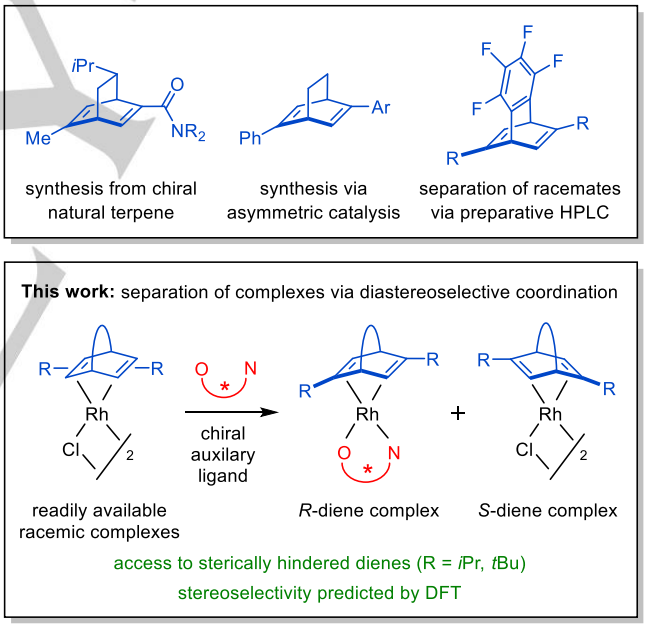

Scheme 1. Some examples of the previously reported chiral diene ligands and our approach to new diene rhodium complexes.

Results and Discussion

Synthesis of catalysts

We chose the tetrafluorobenzobarrelenes (TFB; Scheme 2) as illustrative ligands for our investigation because they strongly bind with transition metals and have interesting electron-acceptor properties.[17] Rhodium complexes with such ligands have been used as catalysts for a variety of transformations.[10,18–25] However, the chiral R_2-TFB ligands (R = Me, Bn, Ph, Fc) have been obtained in 4 steps involving cross-coupling of vinyl triflates and expensive separation of enantiomers by preparative HPLC.[10,26,27]

10.1002/anie.202105179

RESEARCH ARTICLE

We synthesized a series of racemic R_2-TFB ligands (**1a–d**, R = Me, *i*Pr, *t*Bu) in one step by the Diels-Alder reaction of 1,4-substituted benzenes with tetrafluoro-dehydrobenzene C_6F_4, which was generated from C_6F_5Br by BuLi similarly to the literature procedure (Scheme 2).[28] In contrast to the previously used methods,[10] this approach allows for introduction of bulky substituents R, including secondary and tertiary groups, which can improve catalyst selectivity. The structure of the free tetrafluorobenzobarrelene ligand was established by the X-ray diffractions for the first time for the particular member *t*Bu_2-TFB (**1d**).

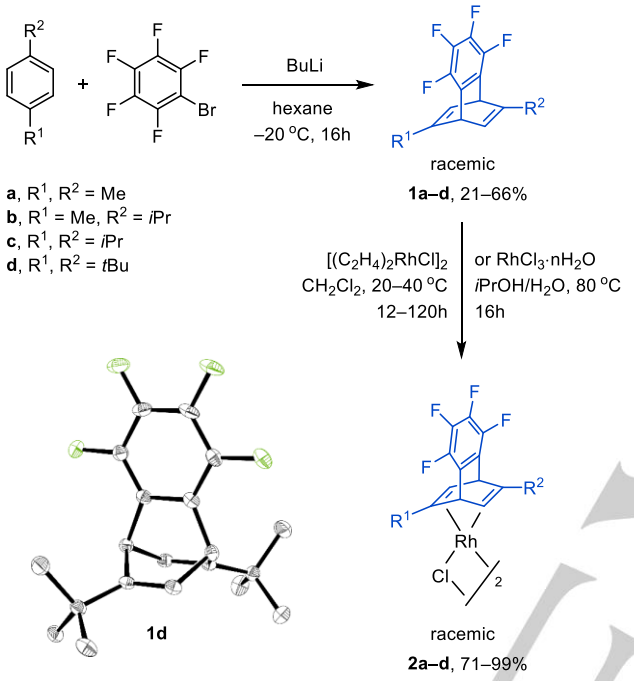

Scheme 2. Synthesis of the tetrafluorobenzobarrelene ligands and their rhodium complexes.

The reactions of dienes **1a–d** with the commercially available rhodium precursor $[(C_2H_4)_2RhCl]_2$ led to the clean replacement of the ethylene ligands and formation of the corresponding racemic complexes $[(R_2\text{-TFB})RhCl]_2$ (**2a–d**) in good to quantitative yields. Noteworthy, the most hindered ligand *t*Bu_2-TFB (**1d**) reacted so slow that heating for several days at 40 °C was necessary to reach the high yields. Less hindered complexes $[(Me_2\text{-TFB})RhCl]_2$ (**2a**) and $[(iPr_2\text{-TFB})RhCl]_2$ (**2c**) were also obtained by heating the ligands directly with $RhCl_3{\times}nH_2O$ in aqueous isopropanol at 80 °C.[29] However, in the case of the bulkier ligand **1d** similar reaction led to the deposition of metallic rhodium, apparently because coordination of the diene was slower than the metal reduction.

The NMR spectra of some of the racemic complexes $[(R_2\text{-TFB})RhCl]_2$ (**2a–d**) in $CDCl_3$ unexpectedly displayed several sets of signals apparently due to the formation of dimeric or oligomeric associates with different chirality of diene ligands.[30] In accordance with this hypothesis, only one set of signals was observed for the enantiomerically pure complexes (*vide infra*). We managed to establish the structures of both homo- and hetero-chiral of dimers for the complex $[(t\text{Bu}_2\text{-TFB})RhCl]_2$ (**2d**) by the X-ray diffraction analysis (Figure 1).

Interestingly, the homo-chiral dimer *R*,*R*-**2d** had a bent structure, that is similar to the parent complex $[(R,R\text{-Me}_2\text{-TFB})RhCl]_2$ (*R*,*R*-**2a**),[26] while analogous bending was absent in the hetero-chiral dimer (see SI), possibly because of the steric repulsion of *t*Bu substituents. The type of dimeric structure, however, had little influence on the chemical behavior of the complexes, because the dimers can dissociate into the monomeric species $[(R_2\text{-TFB})RhCl]$ and react as such. For example, the addition of pyridine converted **2d** into the monomeric adduct $(t\text{Bu}_2\text{-TFB})RhCl(Py)$ (**3**). The X-ray structure of this adduct revealed a notable deviation from the expected square-planar coordination environment of rhodium because of the steric repulsion between two *t*Bu substituents on the one side and chloride and pyridine ligands on the other side.

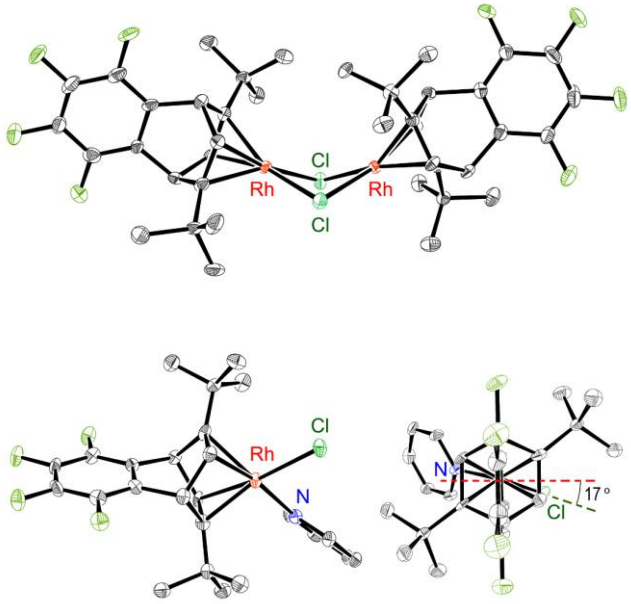

Figure 1. The X-ray structures of the homo-chiral dimeric complex $[(t\text{Bu}_2\text{-TFB})RhCl]_2$ (*R*,*R*-**2d**) (top) and the adduct $(t\text{Bu}_2\text{-TFB})RhCl(Py)$ (**3**) (bottom). Atoms are shown as 50% thermal ellipsoids; independent molecules and hydrogen atoms are omitted for clarity. The green dotted line on the structure of **3** corresponds to N-Rh-Cl plane, the red line shows the positions of Cl and Py ligands expected for the ideal square-planar geometry. Selected distances (Å) for *R*,*R*-**2d**: Rh−Cl 2.382−2.417, C=C 1.395−1.416; for **3**: Rh−Cl 2.3620(14), Rh−N 2.096(4), C=C 1.373(7) and 1.405(7), cf. to C=C 1.327(2) and 1.335(2) for **1d**.

The steric effects of the TFB ligands were quantitatively assessed using the steric maps produced by SambVca 2.1 tool[31] for the calculated structures $(R_2\text{-TFB})Rh(acac)$ (Figure 2). The results clearly showed that the new ligands $i\text{Pr}_2$-TFB (**1c**) and $t\text{Bu}_2$-TFB (**1d**) are more bulky (judging by the total buried volume V_{buried}) and more asymmetric (judging by the difference between V_{buried} of the most and the least occupied quadrants) than the previously used ligands Me_2-TFB[26] and Ph_2-TFB.[20] To the best of our knowledge, the $t\text{Bu}_2$-TFB ligand has the largest total buried volume (V_{buried} = 58%) of all known chiral dienes (compare for example to V_{buried} = 48% for simple 1,5-cyclooctadiene and V_{buried} = 52% for bulky 2,5-diphenyl-norbornadiene).[2]

In order to separate the racemic diene complexes, it was necessary to find a chiral auxiliary ligand L, which would coordinate selectively with one of the enantiomers of $[(R_2\text{-TFB})RhCl]_2$. To do that we calculated the difference in the thermodynamic stability of the corresponding diastereomeric

10.1002/anie.202105179

adducts (*R,R*-*t*Bu$_2$-TFB)Rh(L) and (*S,S*-*t*Bu$_2$-TFB)Rh(L) by DFT methods for various ligands L including L = S-proline (0.03 kcal mol^{-1}), N-isopropyl-*S*-proline (2.77 kcal mol^{-1}), diphenyl-*S*-prolinol (1.05 kcal mol^{-1}), diphenylphosphanyl-*R*-BINOL (0.29 kcal mol^{-1}) and some other (see SI for details). As the result of this screening, we chose isopropyl-salicyloxazoline (*S*-Salox) as one of the most convenient and effective auxiliary ligands (Table 1). *S*-Salox can be easily obtained in one step[32] from the commercially available *ortho*-hydroxybenzonitrile and *S*-valinol, which is derived from the naturally chiral amino acid valine. Salox ligand has been successfully used previously by the group of Prof. Meggers for chromatographic separation of the diastereomers of the octahedral coordination compounds with metal-centered chirality.[33–36]

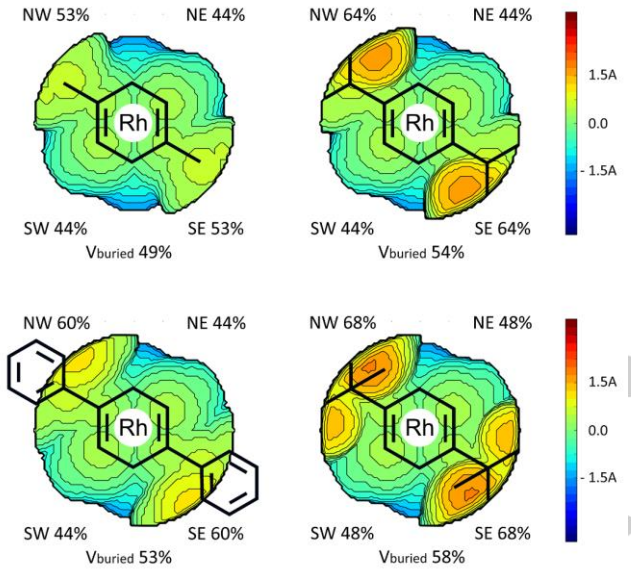

Figure 2. Steric maps of the model complexes (R$_2$-TFB)Rh(acac), R = Me (top left), Ph (bottom left), *i*Pr (top right), *t*Bu (bottom right). V$_{buried}$ indicates the fraction of space occupied by the ligand in the coordination sphere of the metal. NW, NE, SW, SE indicate the fraction of space occupied by ligand in the corresponding quadrants.

DFT calculations at M06L/TZVP level[37] predicted that complexes (*R,R*-R$_2$-TFB)Rh(*S*-Salox) (**4**) with the matching combination of *R,R*-diene and *S*-Salox ligands are significantly more stable than the corresponding diastereomers (*S,S*-R$_2$-TFB)Rh(*S*-Salox) (**5**) with the alternative combination of *S,S*-diene and *S*-Salox (Table 1). The main reason for the different stability is the steric repulsion between R and *i*Pr substituents, which distorts the structure in the second case. Accordingly, the energy difference between the diastereomers increases with the size of the substituents R in the diene ligand from 1.5 kcal mol^{-1} for R = Me to 6.6 kcal mol^{-1} for R = *t*Bu. The calculations also predicted that *S*-Salox auxiliary ligand is able to discriminate the enantiomers of the rhodium complexes with other C$_2$-symmetrical dienes. In particular, the difference in thermodynamic stability of the corresponding diastereomers (*R*-diene)Rh(*S*-Salox) and (*S*-diene)Rh(*S*-Salox) is sufficiently large for separation of complexes with such dienes as 2,5-Ph$_2$-bicyclo-2,2,2-octadiene (2.98 kcal mol^{-1}), 1,5-Ph$_2$-cyclooctadiene (4.77 kcal mol^{-1}), 5,11-Ph$_2$-dibenzo-cyclooctatetraene (4.97 kcal mol^{-1}), as well as some other ligands (see SI for details).

Table 1. The calculated stabilities of the diastereomeric complexes (*R,R*-R$_2$-TFB)Rh(*S*-Salox) (**4**) and (*S,S*-R$_2$-TFB)Rh(*S*-Salox) (**5**).

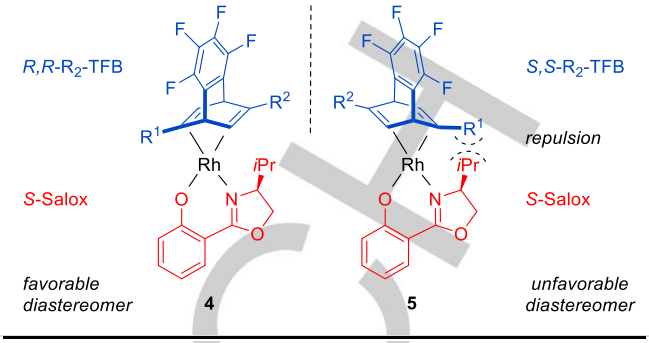

R^1,R^2	ΔG$_f$° of **4** vs **5** (kcal mol^{-1})[a]	Predicted *de* (%) of **4** [b]	Experimental *ee* (%) of *R,R*-**2** [c]
Me$_2$ (**a**)	1.54	86	67
Me, *i*Pr (**b**)	2.57	97	92
^{i}Pr$_2$ (**c**)	3.90	>99	>99
^{t}Bu$_2$ (**d**)	6.58	>99	>99

[a] Calculated difference between ΔG$_f$° of **4** and **5**. [b] Calculated ratio between the diastereomers **4** and **5** assuming the equilibrium with the constant K = exp(−ΔG°/RT). [c] Determined by chiral GS of the diene ligand after the separation (see below).

Experimentally, the target complexes **4a−d** can be synthesized by two possible approaches, differing by whether the starting rhodium complex is chiral or racemic (Scheme 3). The first approach is the stereoselective coordination of the *chiral* rhodium Salox complex with the *racemic* tetrafluorobarrelene ligands **1a−d**. An alternative way is the selective coordination of the *racemic* diene rhodium complexes **2a−d** with the *chiral* Salox anion.

1. L$_2$Rh(*S*-Salox) + 2 *rac*-diene → (*R,R*-diene)Rh(*S*-Salox) + *S,S*-diene + 2L
   1a-d

2. *rac*-[(diene)RhCl]$_2$ + Na[*S*-Salox] → 1/2 (*R,R*-diene)Rh(*S*-Salox) + 1/2 [(*S,S*-diene)RhCl]$_2$ + NaCl
   2a-d

Scheme 3. Two alternative pathways to the chiral complexes (*S,S*-R$_2$-TFB)Rh(*S*-Salox) (**4a−d**).

Following the first approach, we prepared the rhodium precursors L$_2$Rh(*S*-Salox) (L = CO (**6**), C$_2$H$_4$ (**7**)) from *S*-Salox anion and the corresponding chlorides [L$_2$RhCl]$_2$ (Scheme 4). The carbonyl complex **6** was rather inert and reacted with an excess of the diene Me$_2$-TFB (**1a**) only in the presence of Me$_3$N−O to give a mixture of diastereomeric complexes **4a** and **5a** in 6:1 ratio. The replacement of ethylene in the complex **7** proceeded more readily but gave the same mixture with the same ratio. The ratio between diastereomers was apparently determined by their thermodynamic stability rather than by the kinetics of ligand exchange, because it remained unchanged when the reaction of **7** with Me$_2$-TFB was carried out at lower or higher temperatures (0 or 45 °C).

10.1002/anie.202105179

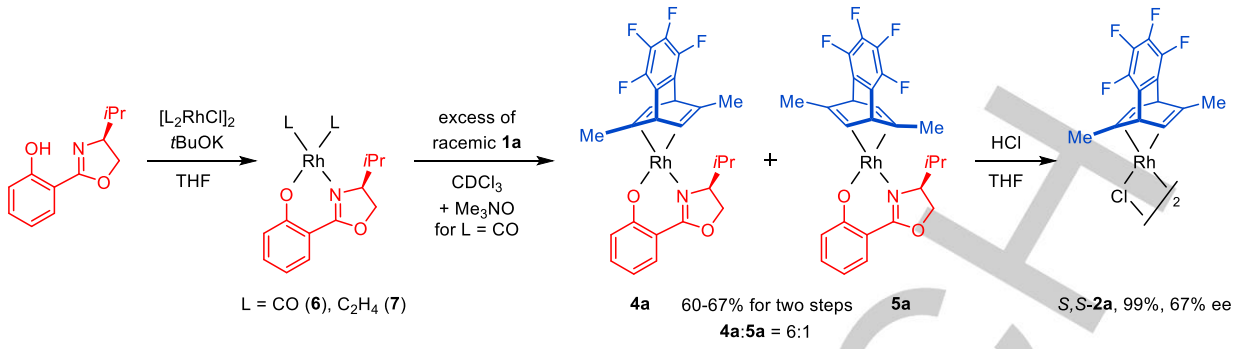

Scheme 4. Coordination of Me2-TFB ligand with Rh-Salox precursors.

Treatment of the resulting mixture of **4a** and **5a** with HCl produced the chloride complex *R,R*-**2a** in almost quantitative yields and with 67% *ee* in good accordance with the observed **4a**:**5a** ratio as well as with the computational predictions (Table 1). Interestingly, the reaction of the racemic diene Me_2-TFB with the rhodium complex containing less hindered methyl-salicyloxazoline ligand $(C_2H_4)_2$Rh(*S*-Me-Salox) gave the mixture of similar diastereomeric complexes (*R,R*-Me_2-TFB)Rh(*S*-Me-Salox) and (*S,S*-Me_2-TFB)Rh(*S*-Me-Salox) with lower 4:1 ratio because of the weaker steric interactions (see SI for details). The reactions of the ethylene complex **7** with the more bulky tetrafluorobarrelene ligands *i*Pr_2-TFB (**1c**) or *t*Bu_2-TFB (**1d**) were expected to have much higher stereoselectivity, but unfortunately they were very slow at 45 °C and led mainly to decomposition products at higher temperatures.

The second approach appeared to be more fruitful. Thus, the reaction of the racemic complex [(*i*Pr_2-TFB)RhCl]$_2$ (**2c**) with 1 equivalent of Na[*S*-Salox] (Rh:Salox ratio = 2:1) selectively produced only one diastereomeric complex (*R,R*-*i*Pr_2-TFB)Rh(*S*-Salox) (**4c**) while the second enantiomer [(*S,S*-*i*Pr_2-TFB)RhCl]$_2$ (*S,S*-**2c**) remained intact (Scheme 5). These complexes can be easily separated by flash chromatography in the presence of morpholine, which prevents acid-catalyzed decomposition of **4c** and forms well-separable adduct with *S,S*-**2c**.[38] The structure of **4c** was confirmed by X-ray diffraction (Figure 3). Both intermediate complexes can be converted into the respective chiral chlorides [(*R,R*-*i*Pr_2-TFB)RhCl]$_2$ (*R,R*-**2c**) and [(*S,S*-*i*Pr_2-TFB)RhCl]$_2$ (*S,S*-**2c**) by treatment with HCl during the work-up procedure; the auxilary *S*-Salox ligand can be also regenerated. For preparative purposes it was more convenient to carry out the reaction with a slightly lower amount of Na[*S*-Salox] (0.9 equiv.). This way the first enantiomeric complex *R,R*-**2c** was directly obtained with >99% enantiomeric purity in 35% yield (50% is theoretically possible). The second enantiomer *S,S*-**2c** was initially obtained in 37% yield and with 84% ee, which was then enhanced to >99% ee by single recrystallization. It is important to emphasize that unlike most known methods[1,2] our approach provides easy access to both enantiomers of the chiral diene complexes. The same procedure allowed us to obtain the more bulky chiral complexes [(*R,R*-*t*Bu_2-TFB)RhCl]$_2$ (*R,R*-**2d**) and [(*S,S*-*t*Bu_2-TFB)RhCl]$_2$ (*S,S*-**2d**) with >99% ee. On the other hand, the less bulky complexes [(*R,R*-Me_2-TFB)RhCl]$_2$ (*S,S*-**2a**) and [(*R,R*-Me-*i*Pr-TFB)RhCl]$_2$ (*S,S*-**2b**) were obtained with a lower enantiomeric excess of 67% and 92% in accordance with the computational prediction (Table 1).

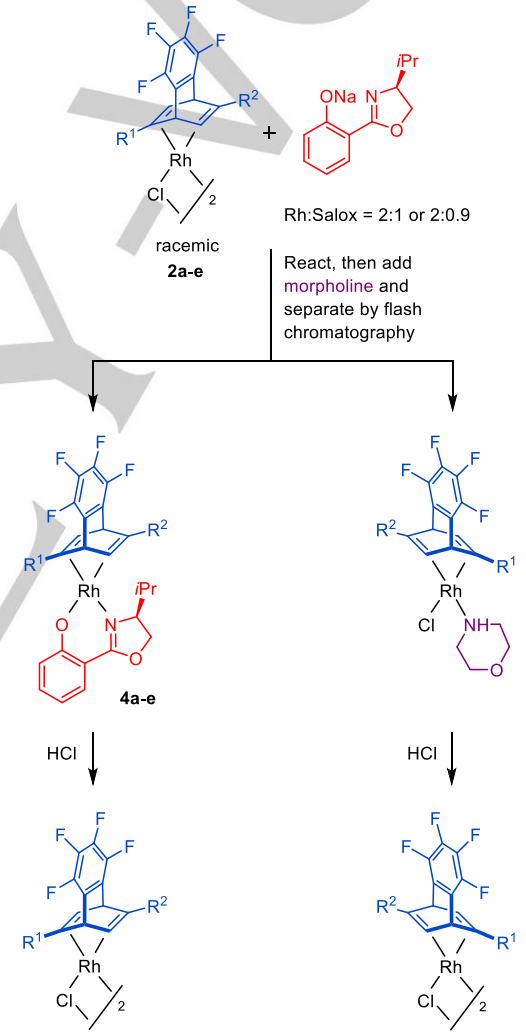

Scheme 5. Separation of enantiomers of [(R_2-TFB)RhCl]$_2$ (**2a–d**) via diastereoselective coordination with *S*-Salox. Enantiomeric purity of the complexes was determined by chiral GS of the corresponding diene ligands after the separation.

10.1002/anie.202105179

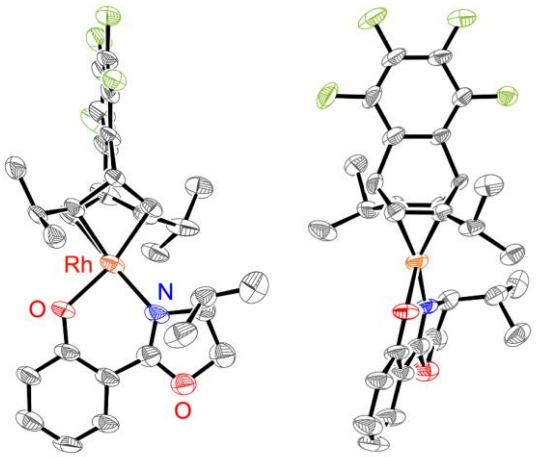

Figure 3. Single-crystal X-ray structure of the complex **4c**. Atoms are shown as 50% thermal ellipsoids, hydrogen atoms are omitted for clarity. Selected distances (Å): Rh−O 2.031(5), Rh−N 2.048(7), C=C 1.390(11) and 1.406(13).

For the demonstration purposes, we also used the developed method for separation of the racemic rhodium complex **2e** with the known Ph_2-TFB ligand.[10] As the result, both enantiomers *R,R*-**2e** and *S,S*-**2e** were obtained in good yields and with 96% and 88% ee, respectively, without application of the preparative chiral HPLC, that have been used previously in the literature.

Catalytic studies

With new chiral complexes in hand, we decided to demonstrate their potential for application as catalysts and had chosen the insertion of diazo compounds into B−H bonds as a showcase reaction. This reaction is interesting and useful because it provides the functionalized boranes that are not accessible via traditional hydroboration. The chiral boranes of this kind can be transformed into various derivatives, such as amines or alcohols, with the retention of stereochemical information.[39–41] Despite these advantages, the asymmetric insertion of diazo compounds into B-H bonds has been described only recently in several reports using closely related diene Rh(I) catalysts,[42] Rh(II) carboxylates,[41] Ru(II) metallacycles,[43] bisoxazoline Cu(I) complexes,[44,45] or engineered cytochrome enzymes.[46,47] We started the investigation with the reaction of *tert*-butyl ester of phenyldiazoacetate (**8a**) with the readily available borane adduct of N-methylpyrrolidine[48] $BH_3{\cdot}N(C_4H_8)Me$ (Table 2). The *t*Bu-substituted catalyst *R,R*-**2d** was tried first, assuming that bulky substituents should provide the highest enantioselectivity. Surprisingly, it reacted very slowly with diazocompound **8a** even at 50 °C, apparently due to the steric overload. Although such hindrance may be excessive for catalytic reactions it may be also helpful for isolation and investigation of reactive intermediates.[49] Fortunately, the *i*Pr-substituted catalyst *R,R*-**2c** (1 mol%) promoted the reaction of **8a** with $BH_3{\cdot}N(C_4H_8)Me$ in DCE already at room temperature giving the desired organoborane product **9a** in 84% yield and with 98% ee. Investigation of the substrate scope demonstrated that this reaction is compatible with both electron-donating (Me, Ph, OMe) and electron-withdrawing (NO_2, Ac, F, CF_3) substituents in the arene ring. The process was a bit slower in the case of sterically hindered substrates such as 2-methylphenyl or 1-napthyl diazoacetates (Table 2, entries 7, 8), which required the use of 1.5 mol% of the catalyst. The enantiomeric excess was almost independent of the substituents in the aromatic ring but correlated with the type ester group. In particular, *tert*-butyl esters of diazocompounds gave products **9a−h** with 97-98% ee, while ethyl esters gave similar products **9i−p** with 91-94% ee. The X-ray diffraction analysis of the compound **9m** confirmed that the catalyst *R,R*-**2c** provided *R*-enantiomer of the product (Figure 4), which correlated with the calculated mechanism of the reaction (*vide infra*). The opposite enantiomer of the catalyst *S,S*-**2c** expectedly produced the second enantiomer of the product *S*-**9j** with almost the same enantiomeric purity 92% ee. Similar selectivity and stereochemistry have been previously observed for the closely related [*R,R*-(diaryl-bicyclo-[2.2.2]-octadiene)RhCl]$_2$ catalyst.[42]

Table 2. Catalytic insertion of diazo compounds into B−H bonds.

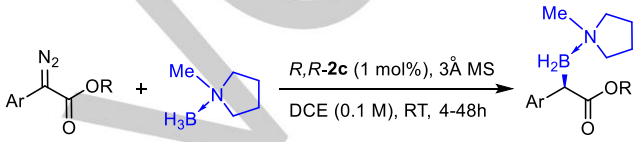

8a-p 1.5 equiv. **9a-p**

#	Ar	R	9	yield (%)[a]	*ee* (%)[b]
1	Ph	*t*Bu	**9a**	84	98
2	4-MeC_6H_4	*t*Bu	**9b**	91	97
3	4-FC_6H_4	*t*Bu	**9c**	98	97
4	4-ClC_6H_4	*t*Bu	**9d**	89	98
5	4-$MeOC_6H_4$	*t*Bu	**9e**	85	97
6	3,4-$(MeO)_2C_6H_3$	*t*Bu	**9f**	84	98
7[c]	2-MeC_6H_4	*t*Bu	**9g**	88	98
8[c]	1-naphtyl	*t*Bu	**9h**	83	89
9	4-$NO_2C_6H_4$	Et	**9i**	86	91
10	3-$NO_2C_6H_4$	Et	**9j**	98	92
11	4-PhC_6H_4	Et	**9k**	93	92
12	4-AcC_6H_4	Et	**9l**	89	92
13	4-BrC_6H_4	Et	**9m**	87	94
14	4-$CF_3C_6H_4$	Et	**9n**	94	91
15	3,5-$F_2C_6H_3$	Et	**9o**	97	93
16	2-fluorenyl	Et	**9p**	95	93
17[d]	3-$NO_2C_6H_4$	Et	*S*-**9j**	99	92

[a] Isolated yield; [b] Determined by chiral HPLC; [c] 1.5 mol% of *R,R*-**2c** catalyst; [d] 1 mol% of *S,S*-**2c** catalyst.

Next, we briefly investigated the catalytic activity of the complex *R,R*-**2c** for analogous insertion of diazocompounds **8** into Si−H bond of triethylsilane (Table 3).[50] This reaction proceeded somewhat slower than the one with boranes but nevertheless gave the corresponding organosilane products **10a−e** in good yields and with high enantiomeric purity. Again the selectivity was

10.1002/anie.202105179

influenced by the ester group and rose from 87% ee for the methyl ester **10a** to 97% ee for the *tert*-butyl ester **10e**. This similarity with B−H insertion suggested that the stereoselectivity was mainly determined by the chirality of a certain carbene intermediate, while the nature of the R_nE−H reagent determined only the speed of the reaction. Accordingly, the more hindered and less nucleophilic triethylsilane reacted slower than amino borane.

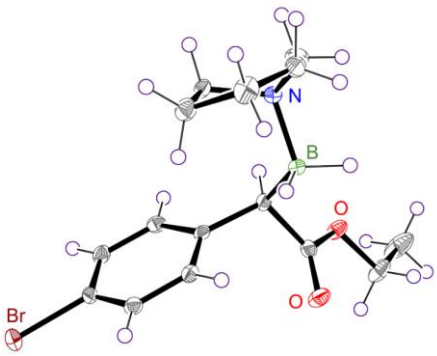

Figure 4. Single-crystal X-ray structure of the borane insertion product **9m** which confirms the stereochemistry of the catalytic reaction. Atoms are shown as 50% thermal ellipsoids, except hydrogens shown as spheres.

Table 3. Catalytic insertion of diazo compounds into Si−H bonds.

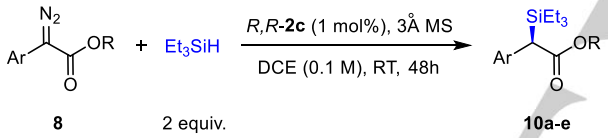

8 2 equiv. **10a-e**

#	Ar	R	**10**	yield (%)[a]	*ee* (%)[b]
1	Ph	Me	**10a**	83	87
2	4-PhC_6H_4	Et	**10b**	82	91
3	3-$NO_2C_6H_4$	Et	**10c**	82	96
4	4-AcC_6H_4	Et	**10d**	78	93
5	3,4-$(MeO)_2C_6H_3$	*t*Bu	**10e**	89	97
6[c]	4-PhC_6H_4	Et	*S*-**10b**	82	88

[a] Isolated yield; [b] Determined by chiral HPLC; [c] 1 mol% of *S,S*-**2c** catalyst.

This hypothesis seemed to be correct for the insertion of diazo compounds into nonpolar E−H bonds such as B−H and Si−H. However, the catalytic reactions of diazoester **8a** with N−H compounds were markedly different (Scheme 6). In particular, the insertion of **8a** into N−H bond of benzamide proceeded cleanly in DCE in the presence of 1 mol% of the catalyst *R,R*-**2c** and gave the desired product **11a** in good yield 70% but without any enantiomeric excess. The analogous reactions with phthalimide and carbazole were less clean and gave the target products **11b** and **11c** in lower yields but with higher stereoselectivity 33 and 42% ee, respectively. Noteworthy, the enantioselectivity was reversed: in contrast to *R*-boranes **9** and *R*-silanes **10**, *S*-enantiomer of the amide **11b** was the major product. It is also interesting to note that the addition of *t*BuOH as co-solvent (10%) strongly improved the stereoselectivity of the insertion giving the carbazole derivative **11c** with 72% ee. *t*BuOH itself did not react with **8a** because of the steric hindrance. At the same time, the less bulky 2-naphthol did react with **8a** in the presence of *R,R*-**2c** but gave only the racemic insertion product 2-(2-naphthyloxy)-phenylacetate.

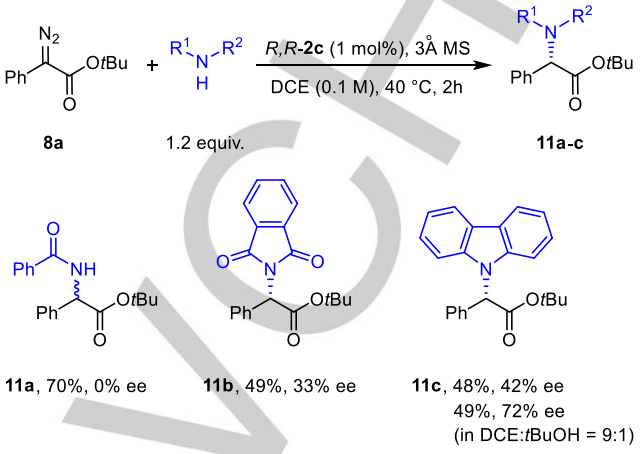

Scheme 6. Catalytic insertion of diazo compounds into N−H bonds.

The effect of *t*BuOH and the differences between the insertion of diazo compounds into B−H, Si−H, N−H, and O−H bonds can be explained by the unified mechanism proposed in accordance with generally accepted concepts[51–53] (Scheme 7). First the dimeric chloride complex *R,R*-**2c** dissociates into monomeric species and reacts with diazoacetate to give the rhodium-carbene intermediate **IM1**. Such carbenes have electrophilic character[54] and therefore the reaction of the carbene **IM1** with B−H and Si−H compounds proceeds as the attack of nucleophilic hydride on the carbon atom followed by the concerted asynchronous formation of the C−B or C−Si bond.[55] On the other hand, the reaction with N-H compounds proceeds as the attack of a nucleophilic nitrogen atom on the carbon atom of **IM1** giving the zwitterion intermediate **IM2**.[52] Intra- or intermolecular proton transfer in **IM2** can lead to the opposite enantiomer of the insertion product as it was observed experimentally. In addition, if the proton transfer is hindered, the intermediate **IM2** can undergo dissociation with the formation of enol-type species and the loss of stereochemical information. Apparently, this is why the stereoselectivity of the reaction was improved by the addition of an external proton source such as *t*BuOH. Further improvement may be possible by finding the more efficient proton transfer reagents (see SI for additional results).[56,57]

We were interested to see whether the DFT calculations can support the proposed mechanism and correctly predict the observed enantioselectivity of the reaction. According to calculations at M06L/TZVP level with solvent corrections for DCE (Scheme 8) the presumed active species [(*R,R*-*i*Pr_2-TFB)RhCl] can reversibly react with diazoester **8a** to give one of two possible adducts ***R*-I** or ***S*-I**.[58] Further removal of N_2 from these intermediates leads to the alternative carbene complexes ***R*-II** or ***S*-II**, which have similar stability but the opposite configuration of the rhodium-bound carbenoid center. The activation barrier for the formation of ***R*-II** is 1.8 kcal mol^{-1} lower than that for ***S*-II**. This energy difference corresponds to the ratio of ***R*-II**:***S*-II** ≈ 95:5, which qualitatively correlates with the experimental formation of

10.1002/anie.202105179

the products *R*-**9** with >90% ee. The simplified explanation for the difference in activation barriers is the unfavorable steric repulsion in the transition state ***S*-TS1** between *i*Pr substituent of the diene ligand and the CO_2tBu group of the diazo ester (see SI for detailed analysis of non-covalent interactions). The formation of carbene complexes ***R*-II** and ***S*-II** is essentially irreversible because of the nitrogen evolution and therefore it determines the stereoselectivity of the whole process.

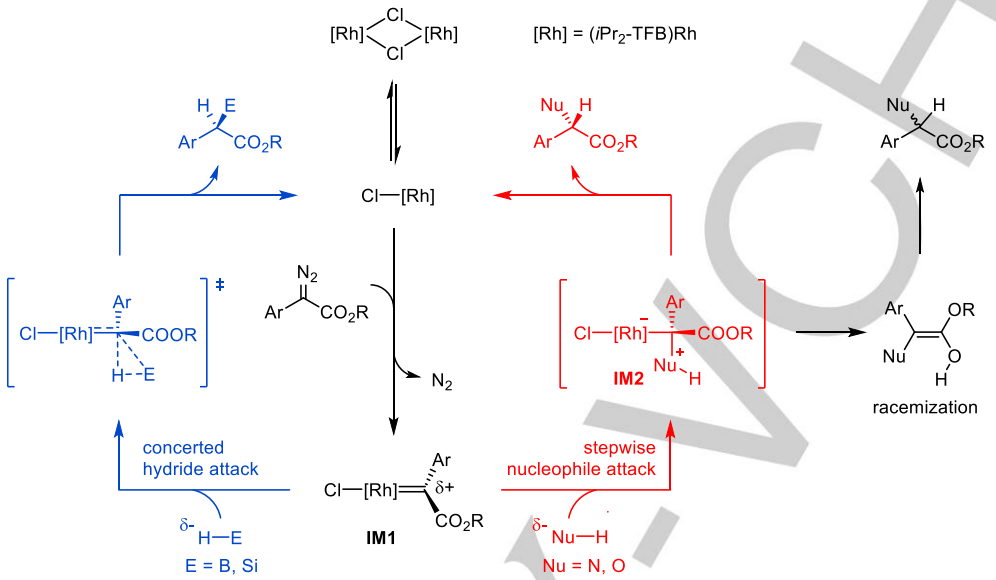

Scheme 7. Proposed mechanism for the catalytic insertion reactions.

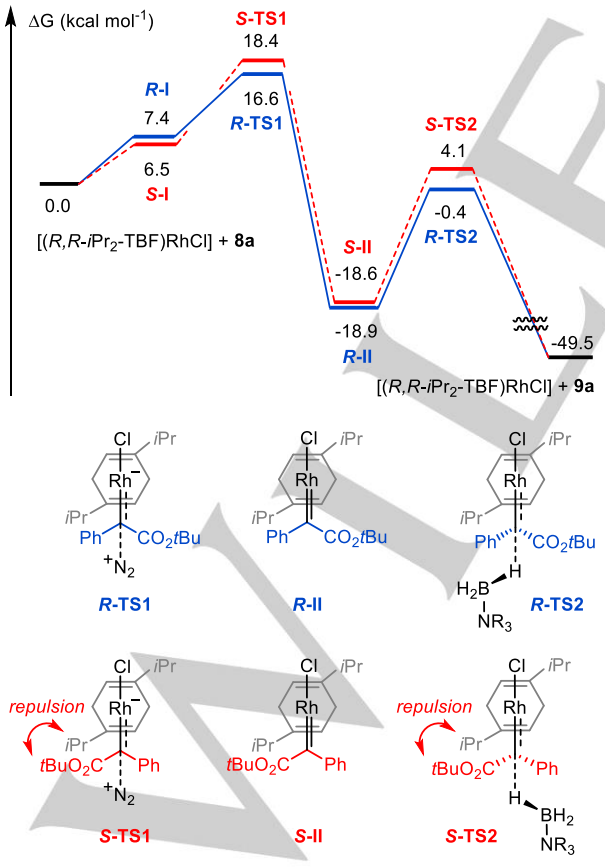

Scheme 8. Free energy diagram of the insertion of diazoester **8a** into B−H bond catalyzed by the active species [(*R*,*R*-*i*Pr$_2$-TFB)RhCl] (at M06L/TZVP level).

For steric reasons the addition of the borane $BH_3{\cdot}N(C_4H_8)Me$ to the carbene complexes ***R*-II** and ***S*-II** can proceed only from one side of the Rh=C bond, which is not blocked by the diene ligand. In accordance with the proposed model, the transfer of a hydride from BH_3 to the carbene carbon occurs first and has a reasonably low activation barrier of 18.5 kcal mol^{-1} (***R*-TS2**) or 22.7 kcal mol^{-1} (***S*-TS2**).[59] Subsequent formation of C−B bond has essentially no barrier according to the potential surface scan and therefore no racemization can occur during this step. Thus the catalyst *R*,*R*-**2c** was correctly predicted to provide *R*-enantiomer of the product **9a**. In contrast to the borane, the reaction of benzamide with the carbene complex ***R*-II** proceeds in a stepwise manner (Scheme 9). The initial nucleophilic attack of the nitrogen[60] via transition state ***R*-TS3** with 18.6 kcal mol^{-1} barrier leads to the zwitterion intermediate ***R*-IV**, which is stabilized by the hydrogen bond between NH and COO*t*Bu groups. Subsequent proton transfer from nitrogen to oxygen via ***R*-TS4** gives complex ***R*-V** with weakly coordinated enol form of the product. The transfer of proton to the carbon atom of ***R*-V** can occur only from the side that is opposite to the rhodium atom and it would lead to the S-enantiomer of the product **11a**. However, the dissociation of ***R*-V** apparently proceeds faster than the proton transfer. It regenerates the active species [(*R*,*R*-*i*Pr$_2$-TFB)RhCl] and gives the racemic form of the product **11a** in accordance with the proposed mechanism on Scheme 7 and experimental observations.

10.1002/anie.202105179

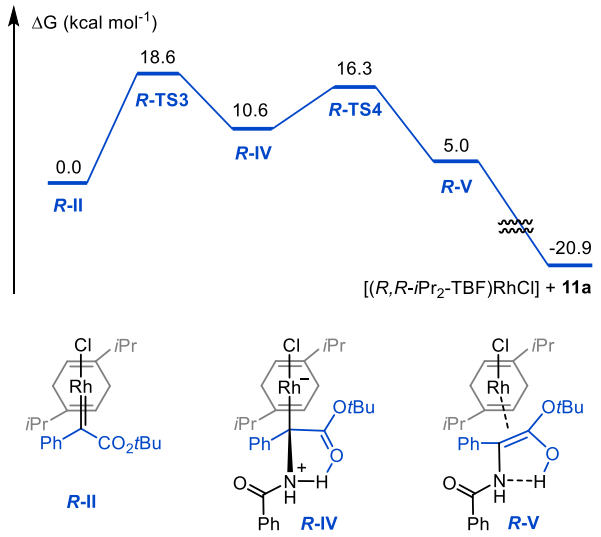

Scheme 9. Free energy diagram of the insertion of the carbene complex **R-II** into N−H bond of benzamide (at M06L/TZVP level).

Conclusion

In summary, we developed a new approach to the rhodium complexes with chiral diene ligands. The method is based on the diastereoselective coordination of one enantiomer from the racemic mixture of the complexes with a chiral auxiliary ligand, which allows for their further separation. Although somewhat similar methods have been employed previously,[35,61–63] the potential of this approach is clearly undeveloped and it can be applied to the complexes of metals other than rhodium and ligands other than dienes. The DFT calculations are especially helpful for this method because they allow one to screen a variety of auxiliary ligands and estimate the selectivity of coordination with sufficient accuracy before the actual synthesis.

New chiral rhodium complexes with exceptionally bulky tetrafluoro-benzobarrelene ligands were synthesized and used as catalysts for asymmetric insertion of diazo esters into B−H and Si−H bonds. A number of boranes and silanes with various functional groups were produced in high yields (79−97%) and enantiomeric purity (87−98% ee). Analogous catalytic insertion of diazo esters into N−H bonds gave the products with opposite chiral configuration thus providing an experimental evidence for the unified mechanism of such transformations. The DFT calculations suggested that enantioselectivity was determined by the structure of the intermediate carbene complex and more specifically by the steric interactions between the ester group and the substituents in the diene ligand. Hopefully, the new rhodium catalysts will find application in other asymmetric transformations.

Acknowledgements

We thank Alexey A. Tsygankov and Dr. Dmitry V. Muratov for their help with analytical measurements. This work was supported by the Russian Science Foundation (grant no. 17-73-20144). X-ray diffraction data were collected with financial support from the Ministry of Science and Higher Education of the Russian Federation using the equipment of the Center for molecular composition studies of INEOS RAS.

Keywords: rhodium • asymmetric catalysis • diene ligands • DFT calculations • carbene insertion

References

[1] C. Defieber, H. Grutzmacher, E. M. Carreira, *Angew. Chem. Int. Ed.* **2008**, *47*, 4482–4502; *Angew. Chem.* **2008**, *120*, 4558–4579.
[2] M. Hirano, N. Komine, E. Arata, T. Gridneva, A. Hatori, N. Kaizawa, K. Kamakura, A. Kuramochi, S. Kurita, S. Machida, H. Okada, A. Sawasaki, T. Uchino, *Tetrahedron Lett.* **2019**, *60*, 150924.
[3] M. M. Heravi, M. Dehghani, V. Zadsirjan, *Tetrahedron Asymmetry* **2016**, *27*, 513–588.
[4] T. Hayashi, K. Yamasaki, *Chem. Rev.* **2003**, *103*, 2829–2844.
[5] T. Yasukawa, H. Miyamura, S. Kobayashi, *Acc. Chem. Res.* **2020**, *53*, 2950–2963.
[6] K. Okamoto, T. Hayashi, V. H. Rawal, *Org. Lett.* **2008**, *10*, 4387–4389.
[7] C. Fischer, C. Defieber, T. Suzuki, E. M. Carreira, *J. Am. Chem. Soc.* **2004**, *126*, 1628–1629.
[8] T. Hayashi, K. Ueyama, N. Tokunaga, K. Yoshida, *J. Am. Chem. Soc.* **2003**, *125*, 11508–11509.
[9] S. Abele, R. Inauen, D. Spielvogel, C. Moessner, *J. Org. Chem.* **2012**, *77*, 4765–4773.
[10] T. Nishimura, H. Kumamoto, M. Nagaosa, T. Hayashi, *Chem. Commun.* **2009**, 5713.
[11] Y. Otomaru, N. Tokunaga, R. Shintani, T. Hayashi, *Org. Lett.* **2005**, *7*, 307–310.
[12] Y. Otomaru, A. Kina, R. Shintani, T. Hayashi, *Tetrahedron: Asymmetry* **2005**, *16*, 1673–1679.
[13] A. Kina, K. Ueyama, T. Hayashi, *Org. Lett.* **2005**, *7*, 5889–5892.
[14] F. Läng, F. Breher, D. Stein, H. Grützmacher, *Organometallics* **2005**, *24*, 2997–3007.
[15] M.-C. Melcher, T. Ivšić, C. Olagnon, C. Tenten, A. Lützen, D. Strand, *Chem. Eur. J.* **2018**, *24*, 2344–2348.
[16] M.-C. Melcher, B. Rolim Alves da Silva, T. Ivšić, D. Strand, *ACS Omega* **2018**, *3*, 3622–3630.
[17] M. A. Esteruelas, L. A. Oro, *Coord. Chem. Rev.* **1999**, *193–195*, 557–618.
[18] T. Nishimura, H. Makino, M. Nagaosa, T. Hayashi, *J. Am. Chem. Soc.* **2010**, *132*, 12865–12867.
[19] T. Nishimura, A. Noishiki, T. Hayashi, *Chem. Commun.* **2012**, *48*, 973–975.
[20] R. Takechi, T. Nishimura, *Chem. Commun.* **2015**, *51*, 8528–8531.
[21] Y. Pan, X. Lu, H. Qiu, T. Hayashi, Y. Huang, *Org. Lett.* **2020**, *22*, 8413–8418.
[22] Y. Huang, T. Hayashi, *J. Am. Chem. Soc.* **2016**, *138*, 12340–12343.
[23] Y. Huang, T. Hayashi, *J. Am. Chem. Soc.* **2015**, *137*, 7556–7559.
[24] K. M.-H. Lim, T. Hayashi, *J. Am. Chem. Soc.* **2015**, *137*, 3201–3204.
[25] M. Umeda, K. Sakamoto, T. Nagai, M. Nagamoto, Y. Ebe, T. Nishimura, *Chem. Commun.* **2019**, *55*, 11876–11879.
[26] T. Nishimura, Y. Ichikawa, T. Hayashi, N. Onishi, M. Shiotsuki, T. Masuda, *Organometallics* **2009**, *28*, 4890–4893.
[27] Separation by crystallization of menthol ethers was also used, but apparently has been abandoned: T. Nishimura, M. Nagaosa, T. Hayashi, *Chem. Lett.* **2008**, *37*, 860–861.
[28] S. C. Cohen, M. L. N. Reddy, D. M. Roe, A. J. Tomlinson, A. G. Massey, *J. Organomet. Chem.* **1968**, *14*, 241–251.
[29] D. S. Perekalin, A. V Kolos, *Mendeleev Commun.* **2021**, *31*, 1–7.
[30] Similar situation has been observed previously for rhodium complexes with diferent chiral ligands: M. Mayr, C. J. R. Bataille, S. Gosiewska, J. A. Raskatov, J. M. Brown, *Tetrahedron Asymmetry* **2008**, *19*, 1328–1332.
[31] L. Falivene, Z. Cao, A. Petta, L. Serra, A. Poater, R. Oliva, V. Scarano, L. Cavallo, *Nat. Chem.* **2019**, *11*, 872–879.
[32] D. Franco, M. Gómez, F. Jiménez, G. Muller, M. Rocamora, M. A. Maestro, J. Mahía, *Organometallics* **2004**, *23*, 3197–3209.

[33] L. Gong, M. Wenzel, E. Meggers, *Acc. Chem. Res.* **2013**, *46*, 2635–2644.
[34] J. Ma, X. Zhang, X. Huang, S. Luo, E. Meggers, *Nat. Protoc.* **2018**, *13*, 605–632.
[35] E. Meggers, *Chem. Eur. J.* **2010**, *16*, 752–758.
[36] E. Meggers, *Eur. J. Inorg. Chem.* **2011**, *2011*, 2911–2926.
[37] D. G. Gusev, *Organometallics* **2013**, *32*, 4239–4243.
[38] Noteworthy, the chromatographic separation of the diastereomers **4a** and **5a** was not successful.
[39] V. K. Aggarwal, G. Y. Fang, A. T. Schmidt, *J. Am. Chem. Soc.* **2005**, *127*, 1642–1643.
[40] J. R. Fulton, V. K. Aggarwal, J. de Vicente, *Eur. J. Org. Chem.* **2005**, *2005*, 1479–1492.
[41] Y. Pang, Q. He, Z.-Q. Li, J.-M. Yang, J.-H. Yu, S.-F. Zhu, Q.-L. Zhou, *J. Am. Chem. Soc.* **2018**, *140*, 10663–10668.
[42] D. Chen, X. Zhang, W.-Y. Qi, B. Xu, M.-H. Xu, *J. Am. Chem. Soc.* **2015**, *137*, 5268–5271.
[43] N. Otog, S. Chanthamath, I. Fujisawa, S. Iwasa, *Eur. J. Org. Chem.* **2021**, *2021*, 1564–1567.
[44] Q. Cheng, S. Zhu, Y. Zhang, X. Xie, Q. Zhou, *J. Am. Chem. Soc.* **2013**, *135*, 14094–14097.
[45] S. Hyde, J. Veliks, B. Liégault, D. Grassi, M. Taillefer, V. Gouverneur, *Angew. Chem. Int. Ed.* **2016**, *55*, 3785–3789; *Angew. Chem.* **2016**, *128*, 3849–3853.
[46] S. B. J. Kan, X. Huang, Y. Gumulya, K. Chen, F. H. Arnold, *Nature* **2017**, *552*, 132–136.
[47] K. Chen, X. Huang, S.-Q. Zhang, A. Z. Zhou, S. B. J. Kan, X. Hong, F. H. Arnold, *Synlett* **2019**, *30*, 378–382.
[48] This type of borane adduct was chosen to achieve better separation of enantiomers of the products by analytical HPLC. Similar results were obtained with more common and commercially available $BH_3{\cdot}NEt_3$.
[49] B. Dutta, B. F. E. Curchod, P. Campomanes, E. Solari, R. Scopelliti, U. Rothlisberger, K. Severin, *Chem. Eur. J.* **2010**, *16*, 8400–9.
[50] For the closely related reaction see: D. Chen, D.-X. Zhu, M.-H. Xu, *J. Am. Chem. Soc.* **2016**, *138*, 1498–1501.
[51] H. M. L. Davies, D. Morton, *Chem. Soc. Rev.* **2011**, *40*, 1857.
[52] D. Gillingham, N. Fei, *Chem. Soc. Rev.* **2013**, *42*, 4918–4931.
[53] H. Keipour, V. Carreras, T. Ollevier, *Org. Biomol. Chem.* **2017**, *15*, 5441–5456.
[54] C. Werlé, R. Goddard, P. Philipps, C. Farès, A. Fürstner, *J. Am. Chem. Soc.* **2016**, *138*, 3797–3805.
[55] X. Li, D. P. Curran, *J. Am. Chem. Soc.* **2013**, *135*, 12076–12081.
[56] B. Xu, S. Zhu, X. Xie, J. Shen, Q. Zhou, *Angew. Chem. Int. Ed.* **2011**, *50*, 11483–11486; *Angew. Chem.* **2011**, *123*, 11685–11688.
[57] Y.-Y. Ren, S.-F. Zhu, Q.-L. Zhou, *Org. Biomol. Chem.* **2018**, *16*, 3087–3094.
[58] The formation of the adducts ***R*-I** and ***S*-I** from [(S,S-iPr2-TFB)RhCl] and diazoester **8a** has favorable enthalpy but unfavorable entropy.
[59] The difference between activation barriers of ***R*-TS2** and ***S*-TS2** also favors the formation of *R*-enantiomer of the product. However, we assume that it is less relevant because the formation of carbene intermediates ***R*-II** and ***S*-II** is irreversible and their ratio is fixed by the difference of ***R*-TS1** and ***S*-TS1**.
[60] Alternative attack of carbene by the hydrogen atom of benzamide has at least 47 kcal mol^{-1} activation barrier according to the potential energy scan.
[61] Z. Zhou, Y. Tan, T. Yamahira, S. Ivlev, X. Xie, R. Riedel, M. Hemming, M. Kimura, E. Meggers, *Chem* **2020**, *6*, 2024–2034.
[62] M. A. Bau, S. Wiesler, S. L. Younas, J. Streuff, *Chem. Eur. J.* **2019**, *25*, 10531–10545.
[63] T. Punniyamurthy, M. Mayr, A. S. Z. Dorofeev, C. J. R. Bataille, S. Gosiewska, B. Nguyen, A. R. Cowley, J. M. Brown, *Chem. Commun.* **2008**, 5092–5094.

10.1002/anie.202105179

WILEY-VCH

RESEARCH ARTICLE

Entry for the Table of Contents

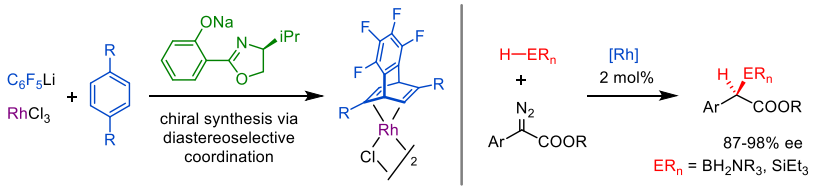

New rhodium complexes with bulky racemic dienes were synthesized and separated into pure enantiomers by diastereoselective coordination with the chiral auxiliary ligand. The optimal structure of the auxiliary ligand and the selectivity of coordination were predicted by DFT calculations. The resulting chiral complexes catalyze the asymmetric insertion of diazoesters into B−H and Si−H bonds.